REPORT DOCUMENTATION PAGE

Form Approved
OMB No. 0704-0188

1. AGENCY USE ONLY (Leave blank)	2. REPORT DATE	3. REPORT TYPE AND DATES COVERED
	April 4, 1995	Final, 1 Jun 92 - 31 Dec 94

4. TITLE AND SUBTITLE
Thermal Decomposition Pathways in Nitramine Propellants

5. FUNDING NUMBERS
ARO MIPR 126-94

6. AUTHOR(S)
F. J. Lovas and R. D. Suenram

7. PERFORMING ORGANIZATION NAME(S) AND ADDRESS(ES)
National Institute of Standards and Technology
Physics Laboratory - Molecular Physics Division, 843
B268 Physics Bldg. (221)
Gaithersburg, MD 20899

8. PERFORMING ORGANIZATION REPORT NUMBER

9. SPONSORING / MONITORING AGENCY NAME(S) AND ADDRESS(ES)
U.S. Army Research Office
P.O. Box 12211
Research Triangle Park, NC 27709-2211

10. SPONSORING / MONITORING AGENCY REPORT NUMBER
ARO 29596.2-CH

11. SUPPLEMENTARY NOTES
The views, opinions and/or findings contained in this report are those of the author(s) and should not be construed as an official Department of the Army position, policy, or decision, unless so designated by other documentation.

12a. DISTRIBUTION / AVAILABILITY STATEMENT
Approved for public release; distribution unlimited.

12b. DISTRIBUTION CODE

13. ABSTRACT *(Maximum 200 words)*

We have investigated intermediates and products in the thermal decomposition of RDX vapor, using a variety of experimental microwave techniques previously employed in our laboratory in studies of pyrolysis decomposition of organic amines. We used microwave spectroscopy to determine the chemical composition of the decomposition of nitramines by pyrolysis methods and identify the products in the thermal decomposition processes. The objective was to determine the validity of proposed decomposition mechanisms, and to identify new reaction products or pathways.

14. SUBJECT TERMS
explosives; microwave; millimeterwave; pyrolysis, spectra

15. NUMBER OF PAGES
44

16. PRICE CODE

17. SECURITY CLASSIFICATION OF REPORT	18. SECURITY CLASSIFICATION OF THIS PAGE	19. SECURITY CLASSIFICATION OF ABSTRACT	20. LIMITATION OF ABSTRACT
UNCLASSIFIED	UNCLASSIFIED	UNCLASSIFIED	UL

THERMAL DECOMPOSITION PATHWAYS IN NITRAMINE PROPELLANTS

FINAL REPORT

F. J. Lovas and R. D. Suenram

March 31, 1995

U. S. Army Research Office

Contract Number 29596-CH

Physics Laboratory

Molecular Physics Division

National Institute of Standards and Technology

Gaithersburg, MD 20899

THE VIEWS, OPINIONS, AND/OR FINDINGS CONTAINED IN THIS REPORT ARE THOSE OF THE AUTHORS AND SHOULD NOT BE CONSTRUED AS AN OFFICIAL DEPARTMENT OF THE ARMY POSITION, POLICY, OR DECISION, UNLESS SO DESIGNATED BY OTHER DOCUMENTS.

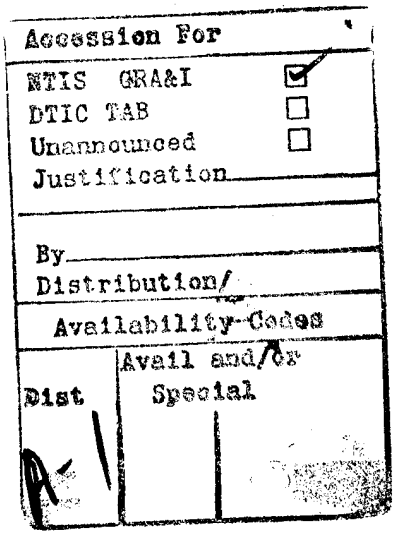

THERMAL DECOMPOSITION PATHWAYS IN NITRAMINE PROPELLANTS

TABLE OF CONTENTS

LIST OF APPENDIXES, ILLUSTRATIONS AND TABLES

Abstract

We have investigated intermediates and products in the thermal decomposition of RDX vapor, using a variety of experimental microwave techniques previously employed in our laboratory in studies of pyrolysis decomposition of organic amines. We used microwave spectroscopy to determine the chemical composition of the decomposition of nitramines by pyrolysis methods and identify the products in the thermal decomposition processes. The objective was to determine the validity of proposed decomposition mechanisms, and to identify new reaction products or pathways.

I. Background

Nitramine propellants[1] are energetic chemical compounds containing nitro groups chemically bound to other nitrogen atoms, i.e., containing fragments of the form N-NO2. RDX (hexahydro-1,3,5-trinitro-1,3,5-triazine) and HMX (octahydro-1,3,5,7-tetranitro-1,3,5,7-tetrazine) are two of the most widely used propellants of this type, and considerable research exists on the macroscopic ignition and combustion properties of RDX and HMX[2-7]. In order to optimize the application of explosives such as RDX and HMX, as well as to devise improved propellants with related chemical properties, a knowledge of the microscopic ignition and combustion behavior of these propellants is required. Obtaining molecular level information on nitramine ignition and combustion in the high-pressure, high-temperature environments typical of actual propellent applications is not easy. It therefore makes sense to pursue an alternative strategy of obtaining information under more controlled laboratory conditions, and transferring this information to the harsher application

environments. We have employed microwave spectroscopy to determine with certainty the chemical composition of many of the products of thermal decomposition of RDX. Thermal decomposition was induced both by simple heating of the sample in a metal nozzle and by a rather gentle thermal pyrolysis technique in which the vapor of RDX is flowed over a heated catalytic substrate.

1. Nitramine Combustion and Decomposition Chemistry

Detailed chemical kinetics mechanisms for ignition and combustion are not well known for any of the energetic propellants. Nevertheless, recent detailed chemical kinetics modelling efforts[8-10] have led to a global understanding for common nitramine propellants which is relatively successful. Melius[8,9] used a model containing 31 chemical species and 137 chemical reactions to reproduce species profiles, flame speed, and pressure dependence for a 0.05 MPa RDX flame. The success of this model suggests that efforts to make it more complete are desirable, and it is in this context that the present study of the chemical composition of early decomposition products should be viewed.

Zhao, Hintsa and Lee[11] used a time-of-flight (TOF) mass spectrometer to detect decomposition products after infrared multiphoton dissociation of RDX in a molecular beam in order to investigate the mechanism of RDX thermal decomposition. They determined photodissociation channels, branching ratios and translational energy distributions. In contrast to the conventional view before their work, i.e., the view that simple bond rupture through loss of NO_2 was the dominant primary channel in RDX thermal decomposition, Zhao, Hintsa and Lee found that the dominant primary channel of photodecomposition is a

concerted symmetric triple fission to produce three $CH_2N_2O_2$ (mass 74) fragments, which subsequently undergo secondary concerted dissociation to produce HCN, H_2CO, HONO (or possibly the isomeric HNO_2) and N_2O. A total of two primary and four secondary dissociation channels were observed.

2. RDX Decomposition - Photolysis Versus Thermal Decomposition

The reaction scheme described above has some parallels in the unimolecular laser infrared multiphoton dissociation (IRMPD) photolysis decomposition scheme for RDX proposed by Zhao, et al.[11] through deconvolution of the time-of flight mass spectra which is illustrated below:

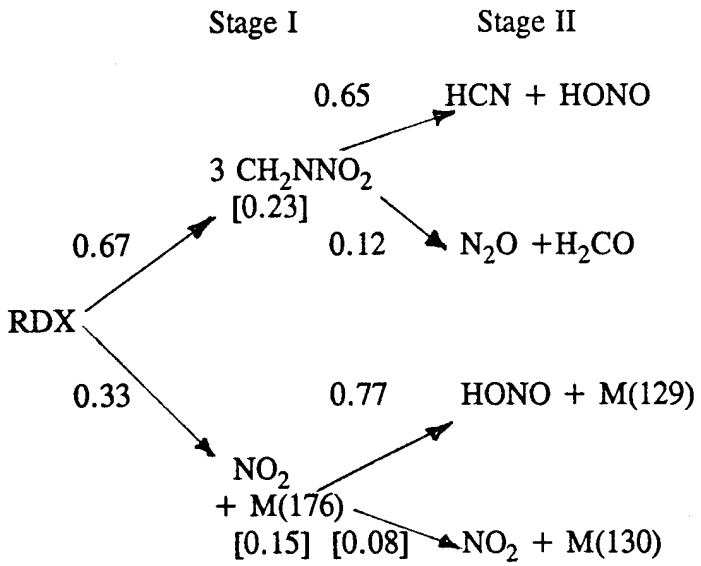

The dominant channel is a concerted triple fission of the RDX ring to produce three $CH_2N_2O_2$ (mass 74) fragments which was identified to be the $CH_3{=}NNO_2$ species. Zhao et al.[11] contend that the dissociation mechanism obtained in IRMPD experiments is the same as that in thermal decomposition experiments on other moderate size systems they have investigated.

Recent pyrolysis studies by Behrens[12-13] on RDX and HDX, which employed thermogravimetric modulated beam and time-of flight mass spectrometry, suggest that decomposition in the liquid phase differs from the gas phase IRMPD experiments. Behrens found that both nitramines form H_2O, N_2O, CH_2O, NO and $(CH_3)NHCHO$. In addition, RDX produces NO_2 and hydroxy-s-triazine from N-N bond breaking while HMX forms $C_2H_6N_2O$ (mass 74), CO and a residue. Behrens argues that the mass 74, with stoichiometry of $C_2H_6N_2O$, is not methyenenitramine ($CH_2N_2O_2$) as suggested in the IRMPD study based on deuterium and ^{15}N labelling experiments, but they do not offer a molecular formula to explain this mass peak. All conceivable structures for this species would require bimolecular reactions since the N=O bond must be ruptured or modified by atom addition. The primary species produced in the thermal decomposition studies of liquid RDX are N_2O, CH_2O, and H_2O, while secondary products are CO, NO, and HCN with minor products C_2H_5NO and $C_2H_6N_2O$. Behrens and Bulusu[14,15] propose the following decomposition paths for liquid RDX at temperatures between 195° C and 215° C:

		Path	Fraction
RDX	$OST^a + H_2O + NO + NO_2$	1	30%
RDX	$NO_2 + H_2CN + 2N_2O + 2CH_2O$	2	10%
RDX [+NO]	$ONDNTA^b$ --> $N_2O + CH_2O$ + other	3	35%
RDX catalyst	$N_2O + CH_2O + NO_2 + NH_2CHO$	4	25%

The first and second pathways are first-order reactions in the decomposition of RDX. Based on their time-of-flight spectra, they concluded that the products HCN, N_2O, HONO, NH_2CHO, and $C_3H_3N_3O$ (oxy-s-triazine) arise only from other decomposition products. The products CO, CH_2O, NO and NO_2 show contributions from RDX and from other decomposition products. No direct evidence for formation of $CH_2{=}NNO_2$ was reported, and the H_2CN species in pathway 2 appears to have been added to account for the chemical

balance based on the RDX formula, $C_3H_6N_6O_6$. Thus, the RDX decomposition experiments studied by the thermogravimetric-mass spectroscopy methods yield dramatically different results than the IRMPD studies and leave many questions unanswered. Mass spectroscopic investigations such as these are clearly an essential tool for studying the decomposition chemistry of nitramine propellants, but mass spectroscopy suffers somewhat as a detection technique from the fact that missing mass peaks, unexpected cracking patterns, complex TOF patterns, and lack of structural information on the products sometimes leads to uncertainties in the interpretation of the identification of the molecular species. It is precisely these uncertainties which might be resolved by microwave studies of the type described here.

II. Experimental Results

The instruments employed are (a) a Stark-modulated millimeterwave spectrometer with computer controlled frequency scanning and equipped with a pyrolysis source, and (b) pulsed-beam Fabry-Perot cavity Fourier-transform microwave (FTMW) spectrometer with a heated nozzle source[19] shown in Figure 1. The frequency coverage of the millimeterwave spectrometer (a) is 18 GHz to 170 GHz using both solid-state and klystron frequency sources, while for the FTMW spectrometer (b) the current frequency range is 6 GHz to 26 GHz. Both spectrometers have computer controlled scan capabilities for broad-band coverage. In the millimeterwave study we used a flow pyrolysis system consisting of a 6 mm o.d. glass tube, filled with granular zeolite material (alumina-silicate) which has been found to produce pyrolytic decomposition at reduced temperatures, heated to 200°-450° C over a length of about 20 cm to study the thermal decomposition products of RDX vapor.

The RDX solid was placed in a small quartz boat 10 cm in length and heated to between 140° and 150° C by a heating tape wrapped around the glass tube surrounding the RDX sample. This system is illustrated in Figure 2a. and 2b.

1. Pulsed-beam Fourier-Transform Experiments

A. Survey of RDX

We have covered the frequency range searched for decomposition products with the FTMW spectrometer with coverage of 6.6 GHz between 8-18 GHz. The RDX sample was placed in a heated reservoir of the pulsed nozzle and pressurized with Ar at 1.2 kPa. Most of the survey was carried out with nozzle temperatures between 140°C and 150°C, and covered the key regions of the known decomposition products as well as searches for methylene nitramine, $CH_2{=}NNO_2$, which is produced in the unimolecular decomposition by Zhao, *et al.*[1]. By far the most intense products are H_2CO and N_2O, followed by HONO, NH_2CHO (formamide) and HNCO. In addition to monomer spectra, several dimers were observed, namely $(H_2O)_2$, Ar-H_2CO, and NH_2CHO-H_2O, since the beam temperature is between 1-5 K. The water appears to originate in the decomposition, since it is not "baked out" of the sample. The species H_2CO, N_2O,and NH_2CHO were sufficiently intense to allow measurement over a range in temperatures (about 140°-190°C) and each showed an exponential growth since the vapor pressure and decomposition are proportional to the temperature. Only one feature has been observed but not assigned. This occurs as a triplet near 9156.35 MHz, the carrier contains H_2CO since it is observed from a pure formaldehyde sample. A summary of the transitions detected in this survey is given in Table I. No

evidence was found for spectra from RDX or methylene nitramine.

B. Structure of Nitromethane-Water

The stimulus for the study of the nitromethane-water complex derives from the theoretical work of Melius[20,21] in which water is found to exert a strong catalytic effect in reducing the barrier to the decomposition of nitramines. Examples are presented for the reactions of nitramine and nitromethane in which "water provides a concerted, cyclic reaction pathway for reduction of the nitro group."[21] The transition state, depicted in Fig. 1b, shows a reduction in the barriers by 27 kcal mol^{-1}. We have studied a number of complexes in which the transition state geometry is replicated by the van der Waals complex at longer distance and strongly suggest that the complexes lie along the reaction coordinate. Examples studied are the complexes for ozone-ethylene[22], ozone-acetylene[23] and ketene-ethylene[24]; the ozone complexes exhibit cyclic van der Waals structures and ketene-ethylene has the heavy atom frames crossed at 90°. Thus, we were interested in determining the geometry the nitromethane-water with respect to the proposed cyclic transition state. The microwave spectrum of the nitromethane-water complex has been studied with FTMW spectrometer. The dominant spectrum is *b*-type with a weaker *a*-type spectrum. Critical to the rotational assignments were well resolved ^{14}N nuclear electric quadrupole transitions, and the incorporation of the pulsed nozzle in one of the mirrors which provided a beam co-axial with the cavity axis to attain linewidths on the order of 2 kHz. In addition to the CH_3NO_2-H_2O species, substitutions of HDO and D_2O in the complex were made, and the CD_3NO_2-H_2O species was also assigned. The molecular structure derived from the moments of

inertia, shown in Fig. 3, has the dipolar axes of each monomer nearly parallel with a center of mass separation of 3.506(7) Å. The complex is quite strongly bonded with a stretching force constant k_s = 9.3 N/m and evidence for two hydrogen bonds of 2.16 Å between an O atom of the NO_2 group and a water H atom, and 2.09 Å between a CH_3 proton and the oxygen atom of water. Unpublished *Ab initio* calculations by W. J. Stevens support this structure. A report describing these results has been accepted for publication in J. Mol. Spectrosc.[25]

2. Pyrolysis Studies of RDX Vapor - Microwave Studies

This experiment involves a conventional microwave absorption spectrometer equipped with a pyrolysis inlet. The RDX sample is heated to a fixed temperature, typically 145° C, and the vapor passes over an alumina-silica catalyst at a higher temperature (200°-450° C) to decompose the vapor. Extensive surveys have been conducted between 54 GHz and 150 GHz with a new synthesizer-locked backwardwave oscillator source from 50-78 GHz and 78-118 GHz from the Russian firm Kvarz. We were able to frequency double the lower frequency unit to survey the region from 123.5-150 GHz. We have assigned less than 10% of these transitions to known species. As in the nozzle experiment, the dominant products are H_2CO and N_2O, with ground and vibrationally excited states detected. Formamide (NH_2CHO) and isocyanic acid (HNCO) are observed and the latter peaks at high catalyst temperature (about 400° C), which suggests that HNCO is produced by decomposition of another product, perhaps formamide, produced at an earlier stage. Several transitions of NO, NO_2 and HONO are observed but are quite weak. The new survey also show more than a dozen lines of CH_3OH. The methanol appears to be an impurity in the RDX sample

since its spectra grows weak the longer the RDX sample is heated, while the other products continue to show strong spectral lines. Our survey contains hundreds unidentified features, and efforts to assign these (or a subgroup of these) to the triple fission product, $CH_2{=}NNO_2$, were unsuccessful in spite of a high quality *ab initio* structure as a guide. Figure 4 shows a calculated spectrum of $CH_2{=}NNO_2$ based on the *ab initio* structure[26] between 75 GHz and 120 GHz; this may be compared to the observed unassigned spectra over the same frequency range in Figure 4. Thus, either $CH_2{=}NNO_2$ is not produced in the RDX vapor decomposition or it is not sufficiently stable to be detected under the conditions of this experiment. A summary of the observed microwave transition for the species identified is given in Table II and the unassigned lines are listed in Appendix I. Behrens and Bulusu[14] report N-methylformamide, CH_3NHCHO (mass 59), as a minor product based on the ion signal at m/z = 58. We have examined and assigned a portion of the millimeterwave spectrum of N-methylformamide with the aid of unpublished lower frequency measurements by R. A. Elzara (PhD Thesis Michigan State University). When comparing the same spectral region surveyed in the RDX pyrolysis, no evidence of N-methylformamide was found.

A. Species X - Assignment of Unidentified Species

During the course of surveying the pyrolysis products of RDX vapor, three lines with resolved Stark effect were observed between 70 GHz and 75 GHz. Each had two Stark shifted components characteristic of *a*-type J = 2-1 R-branch transitions. Subsequent scans at higher harmonic frequencies for the J = 3-2 and J = 4-3 transitions provided additional transitions with the expected Stark effect for this assignment. Table IV lists 12 assigned

transitions for this unknown molecular species which we have labeled "Species-X". The fitted rotational constants are also shown in Table IV. We have tested Species-X by applying a strong magnetic field and see no effect on the spectral lines, thus, it is not paramagnetic and eliminates a radical as a source of the spectrum. The inertial defect, ΔI, is small and positive, which indicates that Species-X is a planar molecule. The magnitude of the rotational constants indicates the species is light and prolate (like formaldehyde or methanol) and the assigned lines all arise from a μ_a dipole moment component. We attempted to locate a *b*-type or *c*-type Q-branch series unsuccessfully. Species-X was observed from virtually every sample of RDX which we pyrolyzed, and also was observed in several sample of HMX pyrolyzed in the same manner as the RDX experiment. Assuming that Species-X is a product of RDX vapor decomposition, and there is no reason to believe otherwise, it is constrained to be composed of $H_nC_xN_yO_z$ where n, x, y, and z are integers, since the empirical formula of RDX is $C_3H_6N_6O_6$. Further, every known species having three first row atoms (C, N or O) in any combination has B and C rotational constants near 10 to 13 GHz, much smaller that Species-X. Thus, we are led to believe that Species-X can contain only two of these first row atoms. In Table V we have constructed a chart of all pairs of C, N, and O and then adding H's until the valence bonding is saturated. At the bottom of Table V rotational constants from microwave spectral analysis are shown. From the magnitude of the A rotational constant (140 GHz) for Species-X, it is clear that 3 hydrogen atoms off the heavy atom axis (H_2NOH or $CH_2{=}NH$) are too few and 5 hydrogen atoms are too many (CH_3NH_2), while 4 hydrogen atoms are close (H_2NNH_2 and CH_3OH). The methylamine B and C rotational constants are slightly larger (10%) than Species-X, which is true of the

other saturated forms of the diatoms. The puzzle is in the fact that all of the stable species (radicals were not considered based on the results of the paramagnetic test) we can conceive of are listed in Table V and each of these either has no microwave spectrum (H_nC_2 species) due to a lack of dipole moment, or has already been assigned, i.e. we know the rotational constants, and these do not explain Species-X. Thus, our best guess for the formula of Species-X is H_4XY, where X and Y = C, N, or O.

B. Temperature profiles

Temperature profiles of the identified species whose intensities were sufficiently strong were measured by keeping the temperature of the RDX sample constant and increasing (or decreasing) the temperature of the catalyst pyrolysis zone. In Figure 6 profiles for HCN, H_2CO, N_2O, CO, HNCO, and Species-X are shown. The results are rather poor due to the slow flow employed in order to maintain a constant pressure in the absorption cell. With increasing temperature the cell pressure increased due to more decomposition, while the opposite occurs when starting at the highest temperature and decreasing the temperature. However, a general trend is evident: The N_2O, H_2CO and Species-X were strongest at pyrolysis temperatures between 250° C and 300° C, while HCN and HNCO had a peak intensity between 400° C and 450° C. The CO species was rather constant over the whole range and NO_2 shows increasing intensity up to 450° C. Thus, it would appear that Species-X, H_2CO and N_2O appear as first stage products, while HCN and HNCO are second stage products, i.e. result from pyrolysis of first stage products. Very likely HNCO comes from pyrolysis of formamide (NH_2CHO). These results are in agreement with those of Behrens and Bulusu[14]. It is interesting that species-X correlates with the first stage products.

III. Conclusions

The unimolecular laser infrared multiphoton dissociation (IRMPD) photolysis decomposition scheme for RDX proposed by Zhao, et al.[1] showed that the dominant channel is a concerted triple fission of the RDX ring to produce three $CH_2N_2O_2$ (mass 74) fragments and identified it to be the $CH_2{=}NNO_2$ species. Behrens and Bulusu[2] have studied the decomposition of liquid RDX and several isotopically labeled species and concluded that four pathways occur in the liquid including a surface catalyzed path in which NH_2CHO is produced. Several large species were initially formed, namely, oxy-s-triazine ($C_3H_3N_3O$) and 1-nitroso-3,3-dinitrohexahydro-s-triazine, whose structure and microwave spectra are unknown. The observed products in our experiments correlate better with the mechanism of Behrens and Bulusu, although several differences were found. We did not observe N-methylformamide attributed to mass peak m/z = 58, and we detected several species not reported in the mass spectrometry study, namely, Species-X, HCOOH, HNCO, and possibly acetaldehyde, CH_3CHO. Most of the spectral lines observed in the millimeterwave survey remain unassigned. Perhaps these may be attributed to the two species detected by mass spectrometry, OST (oxy-s-triazine) and ONDNTA (1-nitroso-3,5-dinitrohexahydro-s-triazine), whose microwave spectrum is unknown. Cosgrove and Owen[27] reported the detection of formic acid in the decomposition of RDX vapor at 195° C via a chemical test. It might be noted that HCOOH has the same mass (46) as NO_2 and CH_3CHO has the same mass (44) as N_2O, thus, the presence in the mass spectrum might be masked by this other known products.

REFERENCES

1. T. L. Boggs, "The Thermal Behavior of Cyclotrimethylene-trinitramine(RDX) and Cyclotetramethylene-tetranitramine (HMX)," in Fundamentals of Solid-Propellant Combustion, K. K. Kuo and M. Summerfield, Eds., Prog. in Aeronautics and Astronautics **90**, 121 (1984).

2. R. A. Fifer, "Chemistry of Nitrate Ester and Nitramine Propellants," in Fundamentals of Solid-Propellant Combustion, K. K. Kuo and M. Summerfield, Eds., Prog. in Aeronautics and Astronautics **90**, 177 (1984).

3. M. A. Schroeder, "Critical Analysis of Nitramine Decomposition Data: Activation Energies and Frequency Factors for HMX and RDX Decomposition," Report No. BRL-TR-2673, Ballistics Research Laboratory, Aberdeen Proving Ground, Aberdeen, Maryland MD (September 1985); M. A. Schroeder, "Critical Analysis of Nitramine Decomposition Data: Product Distributions from HMX and RDX Decomposition," Report No. BRL-TR-2659 (June 1985).

4. M. D. Cook, *J. Energ. Materials* **5**, 257 (1987).

5. B. Suryanarayana, R. Graybush, and J. R. Autera, *Chem. and Ind.* 2177 (1967).

6. F. I. Dubovitskii and B. L. Korsunski, *Russian Chem. Rev.* **50**, 958-978 (1980) [Uspeki Khimii **50**, 1828-1871 (1981)].

7. R. W. Shaw, Jr. and G. F. Adams, Eds, "Diagnostics for Propellant Ignition," Army Research Office (June 1985), DTIC No. B093719.

8. C. F. Melius, "Thermochemical Modeling: I. Application to Decomposition of Energetic Materials," in Chemistry and Physics of Energetic Materials, S. N. Bulusu, ed., Kluwer Academic Publishers, Dordrecht, The Netherlands, p21-49 (1990).

9. C. F. Melius, "Thermochemical Modeling: II. Application to Ignition and Combustion of Energetic Materials," in Chemistry and Physics of Energetic Materials, S. N. Bulusu, ed., Kluwer Academic Publishers, Dordrecht, The Netherlands, p51-78 (1990).

10. R. Hatch, "Chemical Kinetics Modeling of HMX Combustion," presented at the 24th JANNAF Combustion Meeting, Monterey Calif. (1987).

11. X. Zhao, E. J. Hintsa and Y. T. Lee, "Infrared multiphoton dissociation of RDX in a molecular beam," *J. Chem. Phys.* **88**, 801 (1988).

12. R. Behrens, "The Application of Simultaneous Thermogravometric Modulated Beam

Mass Spectrometry and Time-of-Flight Velocity Spectra Measurements to the Study of the Pyrolysis of Energetic Materials," in Chemistry and Physics of Energetic Materials, S. N. Bulusu, ed., p327-346.

13. R. Behrens, "Thermal Decomposition of HMX and RDX: Decomposition Processes and Mechanisms Based on STMBMS and TOF Velocity-spectra Measurements," in Chemistry and Physics of Energetic Materials, S. N. Bulusu, ed., p347-368.

14. R. Behrens, Jr., and S. Bulusu, "Thermal Decomposition of Energetic Materials. 3. Temporal Behaviors of the Rates of Formation of the Gaseous Pyrolysis Products from Condensed-Phase Decomposition of 1,3,5-Trinitrohexahydro-s-triazine," *J. Phys. Chem.* **96**, 8877 (1992).

15. R. Behrens, Jr., and S. Bulusu, "Thermal Decomposition of Energetic Materials. 4. Deuterium Isotope Effects and Isotopic Scrambling (H/D, $^{13}C/^{18}O$, $^{14}N/^{15}N$ in Condensed-Phase Decomposition of 1,3,5-Trinitrohexahydro-s-triazine," *J. Phys. Chem.* **96**, 8891 (1992).

16. F. J. Lovas, F. O. Clark and E. Tiemann, "Pyrolysis of Ethylamine. I. Microwave Spectrum and Molecular Constants of Vinylamine," *J. Chem. Phys.* **62**, 1925 (1975).

17. F. J. Lovas, R. D. Suenram, D. R. Johnson, F. O. Clark and E. Tiemann, "Pyrolysis of Ethylamine II. Synthesis and Microwave Spectrum of Ethylidenimine ($CH_3CH=NH$)," *J. Chem. Phys.* **72**, 4964 (1980).

18. F. J. Lovas, "Application of Microwave Spectroscopy to Chemical Analysis," *ISA Transactions* **14**, 145 (1975).

19. F. J. Lovas, and R. D. Suenram, "Pulsed Beam Fourier Transform Microwave Measurements on OCS and Rare Gas Complexes of OCS with Ne, Ar, and Kr," *J. Chem. Phys.* **87**, 2010 (1987); R. D. Suenram, F. J. Lovas, G. T. Fraser, J. Z. Gillies, C. W. Gillies, and M. Onda, "Microwave Spectrum, Structure, and Electric Dipole Moment of Ar-CH_3OH," *J. Mol. Spectrosc.* **137**, 127 (1989).

20. C. F. Melius, in Chemistry and Physics of Energetic Materials (ed. S. Bulusu), pp. ASI **309**, NATO.

21. C. A. Melius, *Phil. Trans. R. Soc. Lond.* A **339**, 365-376 (1992).

22. J. Z. Gillies, C. W. Gillies, R. D. Suenram, F. J. Lovas, and W. Stahl, *J. Amer. Chem. Soc.* **111**, 3073-3074 (1989); C. W. Gillies and J. Z. Gillies, R. D. Suenram, F. J. Lovas, E. Kraka, and D. Cremer, *J. Am. Chem. Soc.* **113**, 2412-2421 (1991).

23. J. Z. Gillies, C. W. Gillies, F. J. Lovas, K. Matsumura, R. D. Suenram, E. Kraka,

and D. Cremer, *J. Am. Chem. Soc.* **113**, 6408-6415 (1991).

24. C.W. Gillies, J.Z. Gillies, F.J. Lovas, and R.D. Suenram, *J. Am. Chem. Soc.* **115**, 9253-62 (1993).

25. F.J. Lovas, N. Zobov, G.T. Fraser, and R.D. Suenram, *J. Mol. Spectrosc.* **171**, xxx (1995).

26. R.C. Mowrey, M. Page, G.F. Adams, and B.H. Lengsfield III, *J. Chem. Phys.* **93**, 1857 (1990).

27. J.D. Cosgrove and A.J. Owen, *Combustion and Flame* **22**, 13 (1974).

LIST OF PUBLICATIONS

F.J. Lovas, N. Zobov, G.T. Fraser, and R.D. Suenram, *J. Mol. Spectrosc.* **171**, xxx (1995).

LIST OF PARTICIPATING SCIENTIFIC PERSONNEL

N. Zobov, NIST Guest Worker
M-Yu. Tretyakov, NIST Guest Worker
Institute of Applied Physics
Nizhny Novgorod, Russia

G.T. Fraser, NIST staff

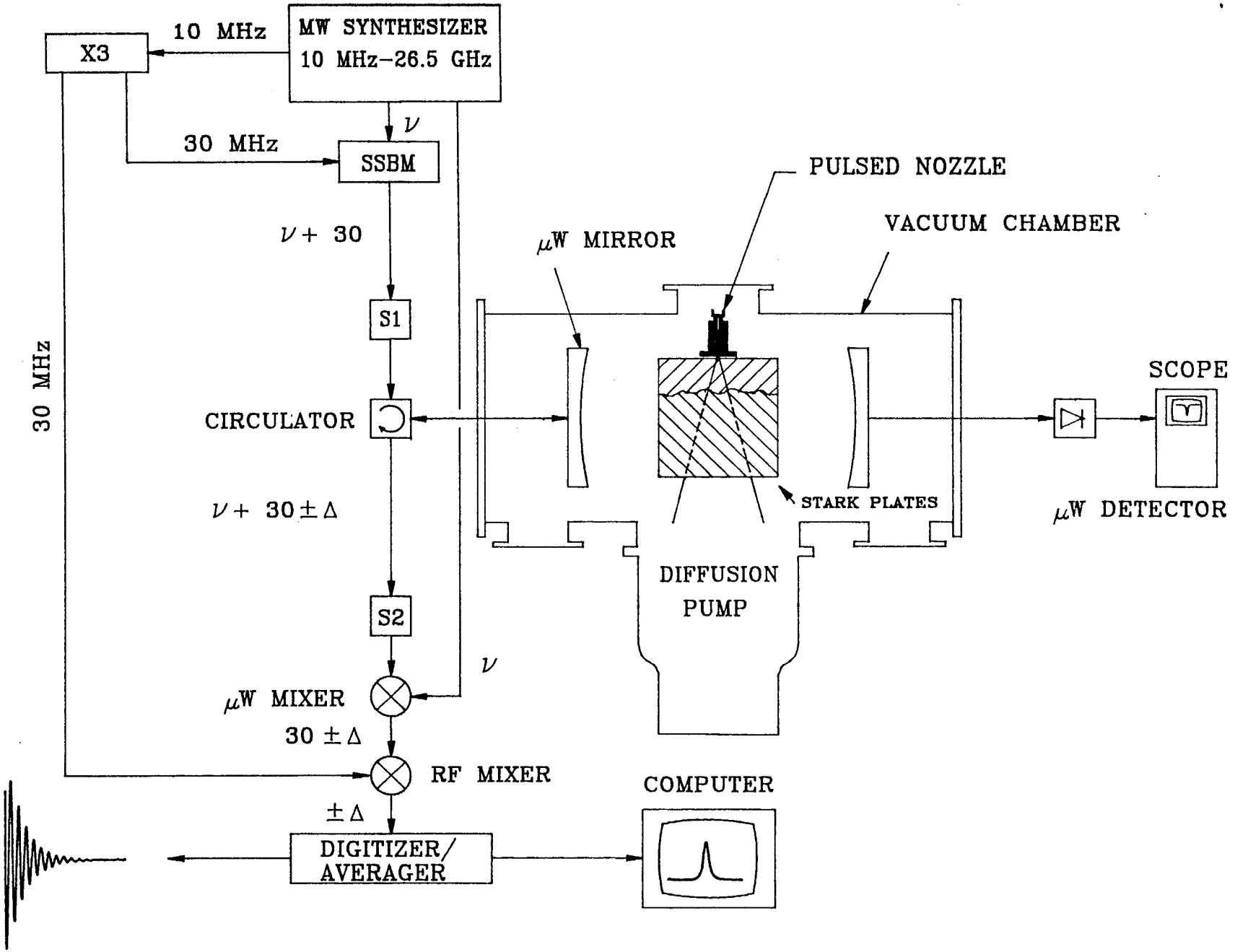
10 MHz
MW SYNTHESIZER
10 MHz–26.5 GHz
X3
ν
30 MHz
SSBM
PULSED NOZZLE
VACUUM CHAMBER
ν + 30
μW MIRROR
S1
30 MHz
SCOPE
CIRCULATOR
STARK PLATES
ν + 30 ± Δ
μW DETECTOR
DIFFUSION
PUMP
S2
ν
μW MIXER
30 ± Δ
RF MIXER
COMPUTER
± Δ
DIGITIZER/
AVERAGER

FIG. 1

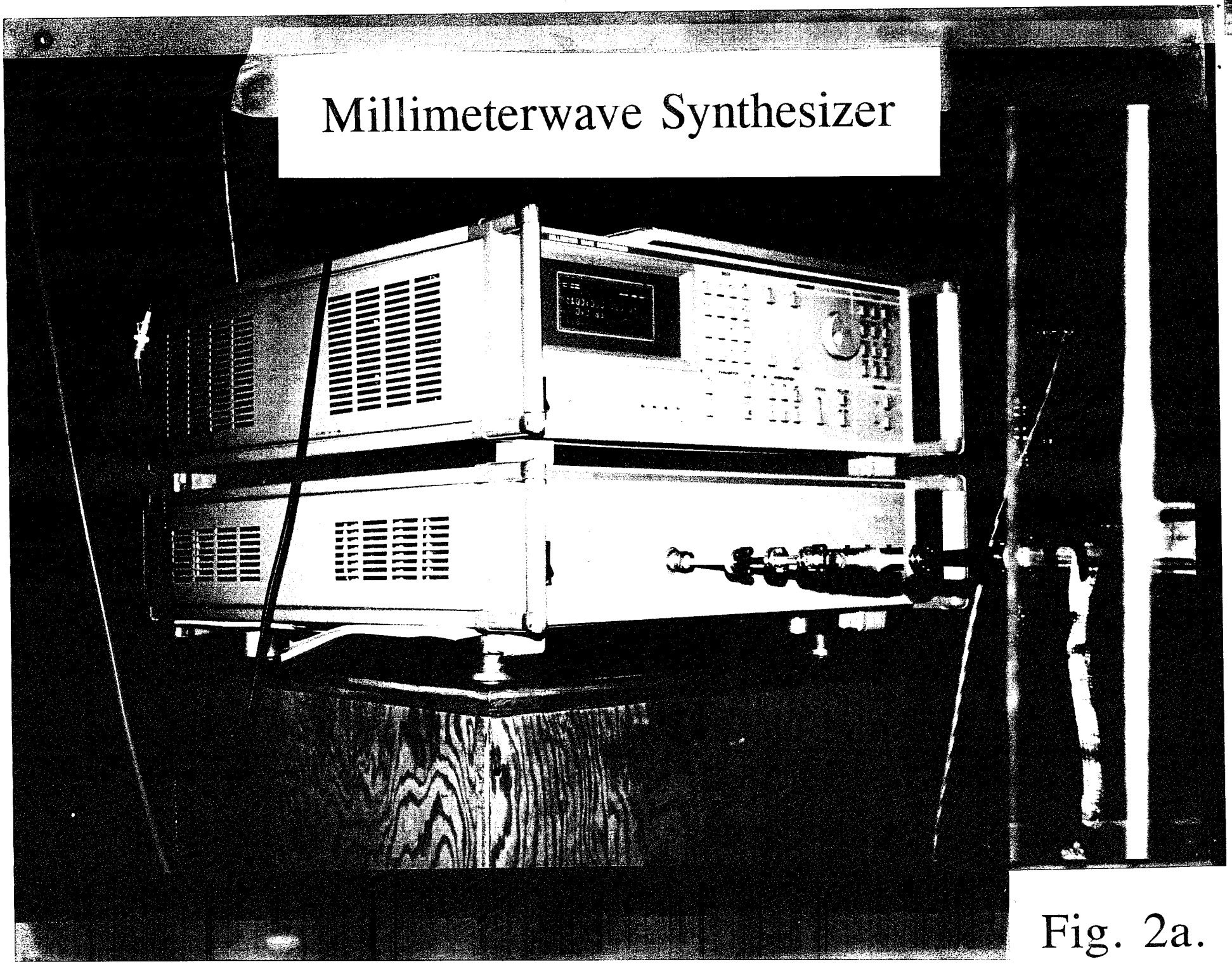

Fig. 2a.

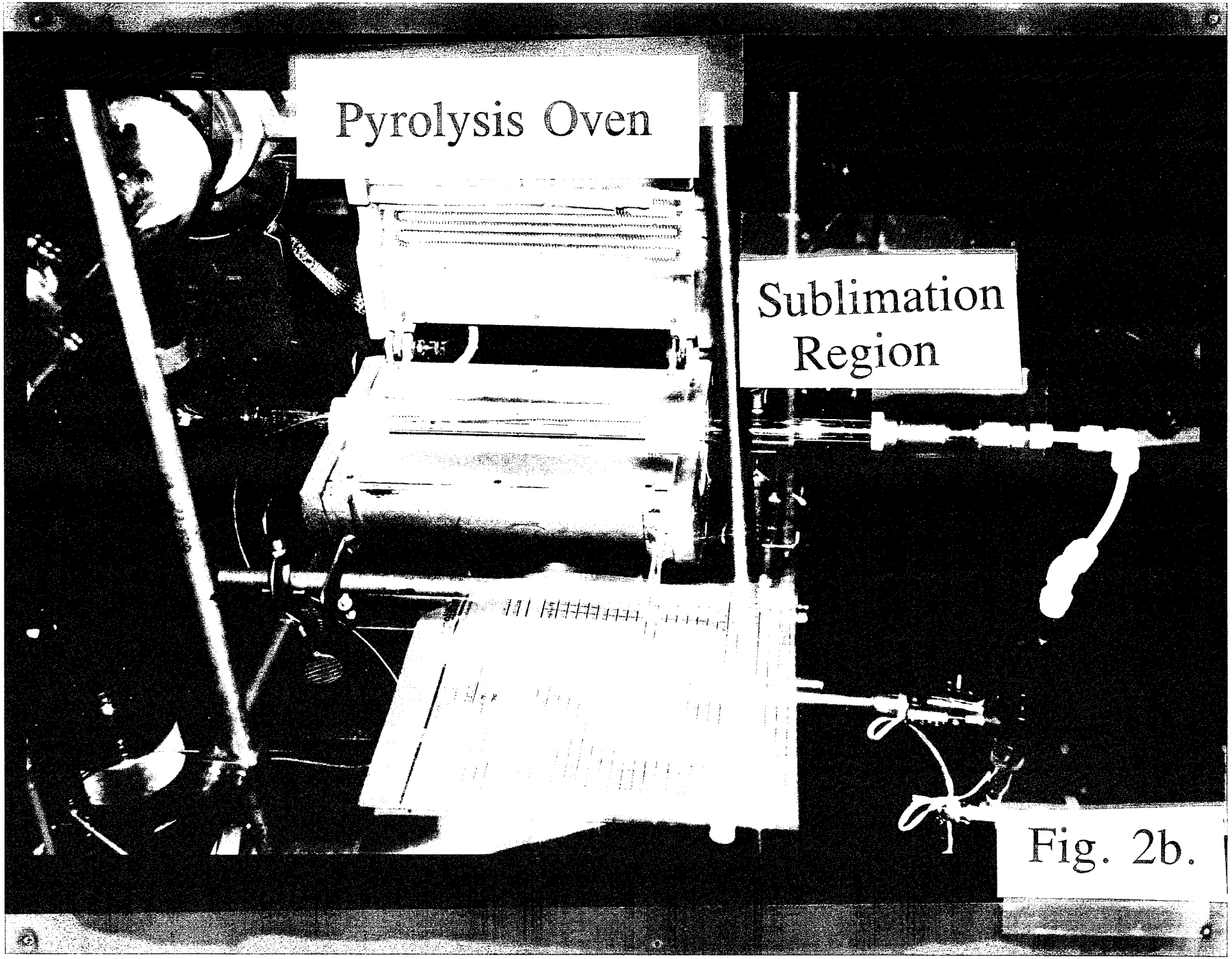

Fig. 2b.

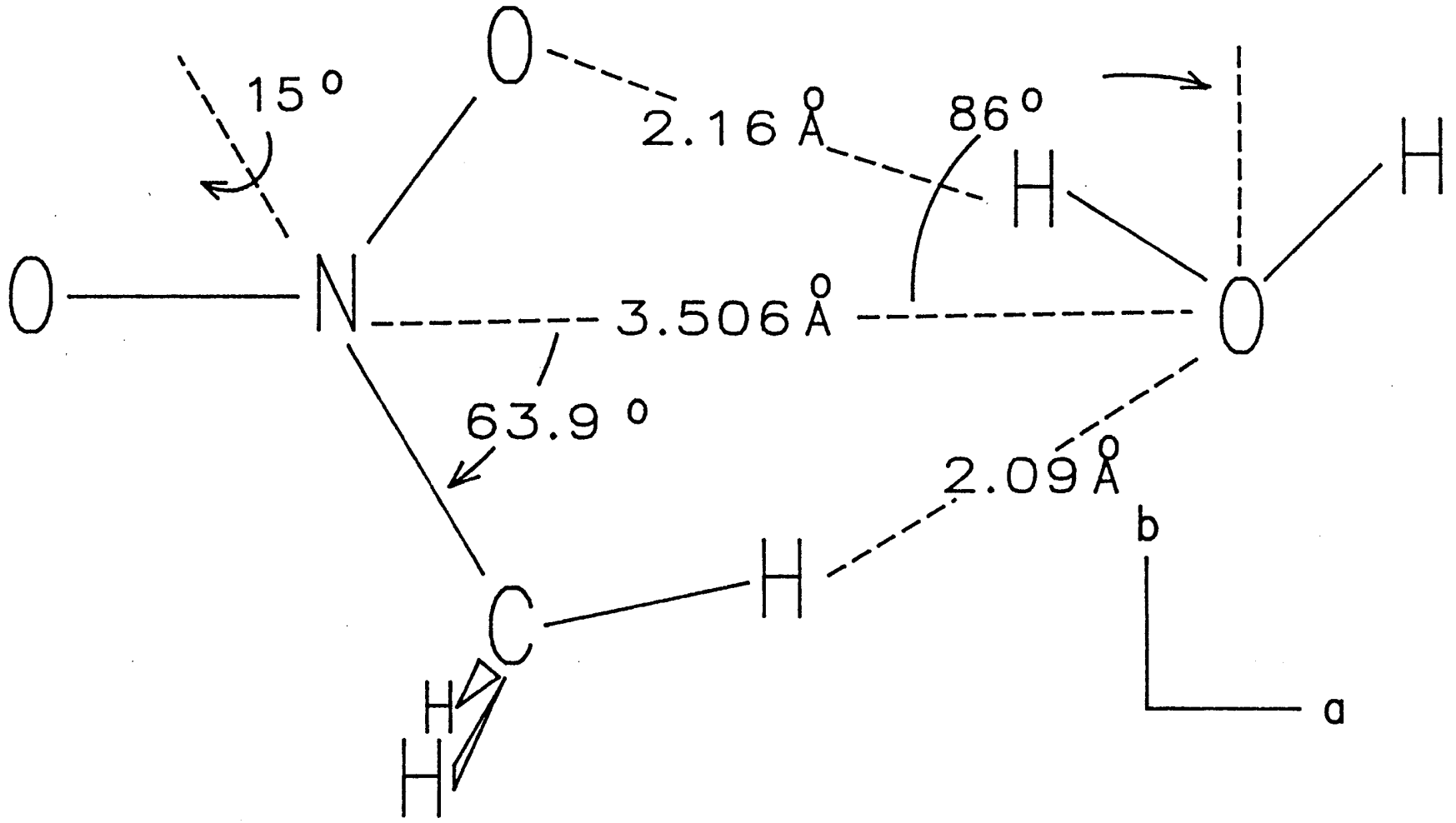

Fig 3

Calculated

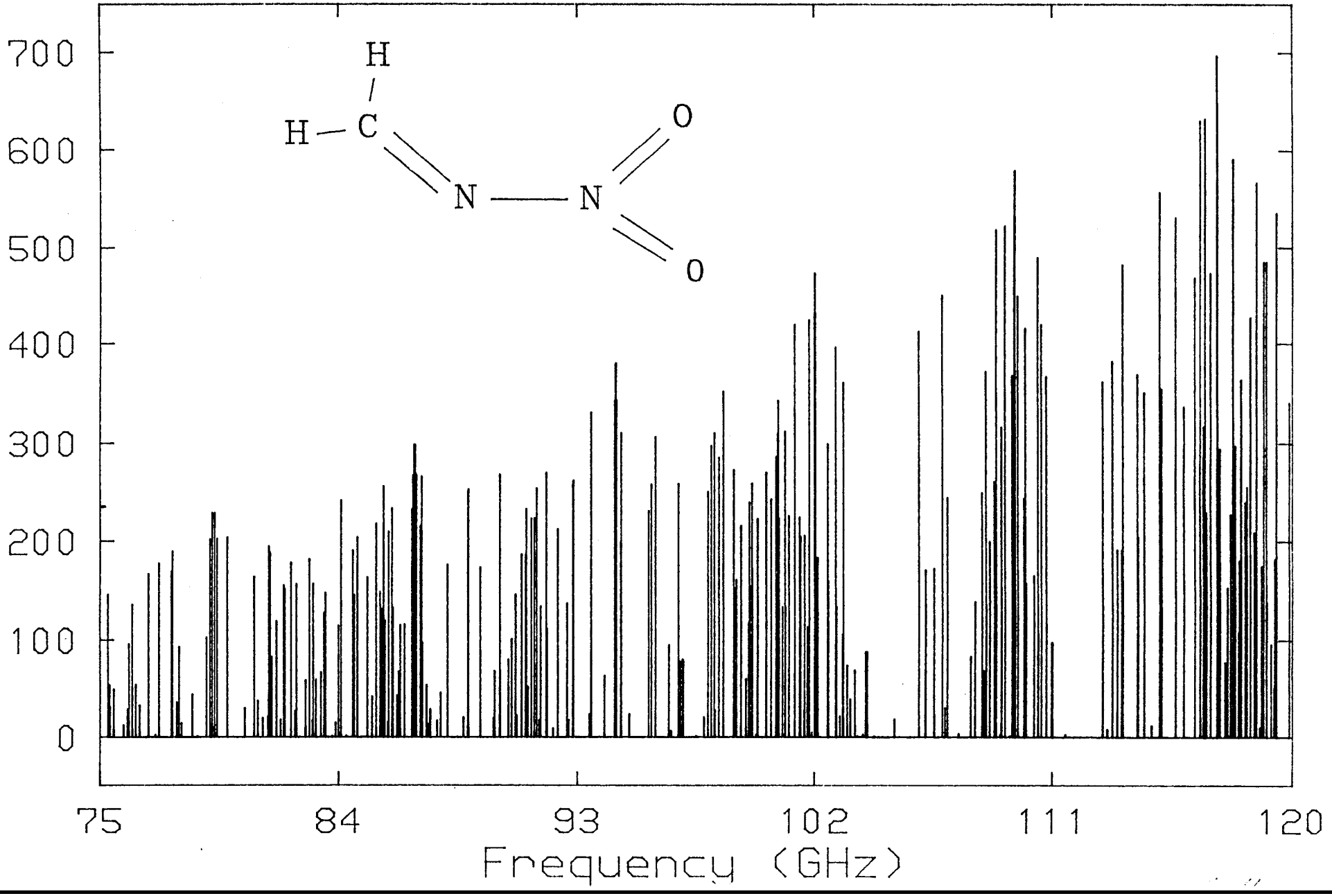
H
H
C
N
N
O
O
700
600
500
400
300
200
100
0
75
84
93
102
111
120
Frequency (GHz)

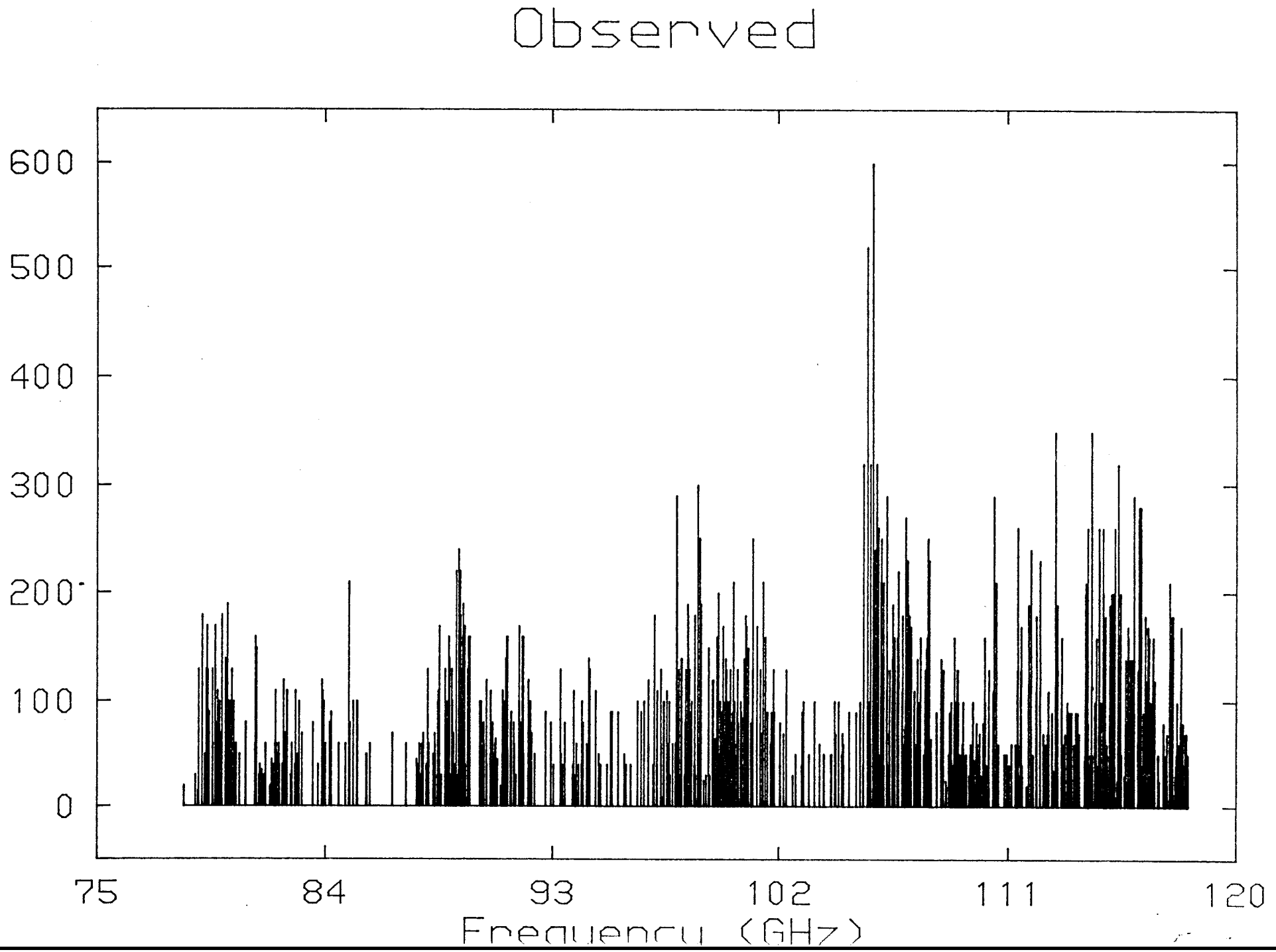
Observed
600
500
400
300
200
100
0
75
84
93
102
111
120
Frequency (GHz)

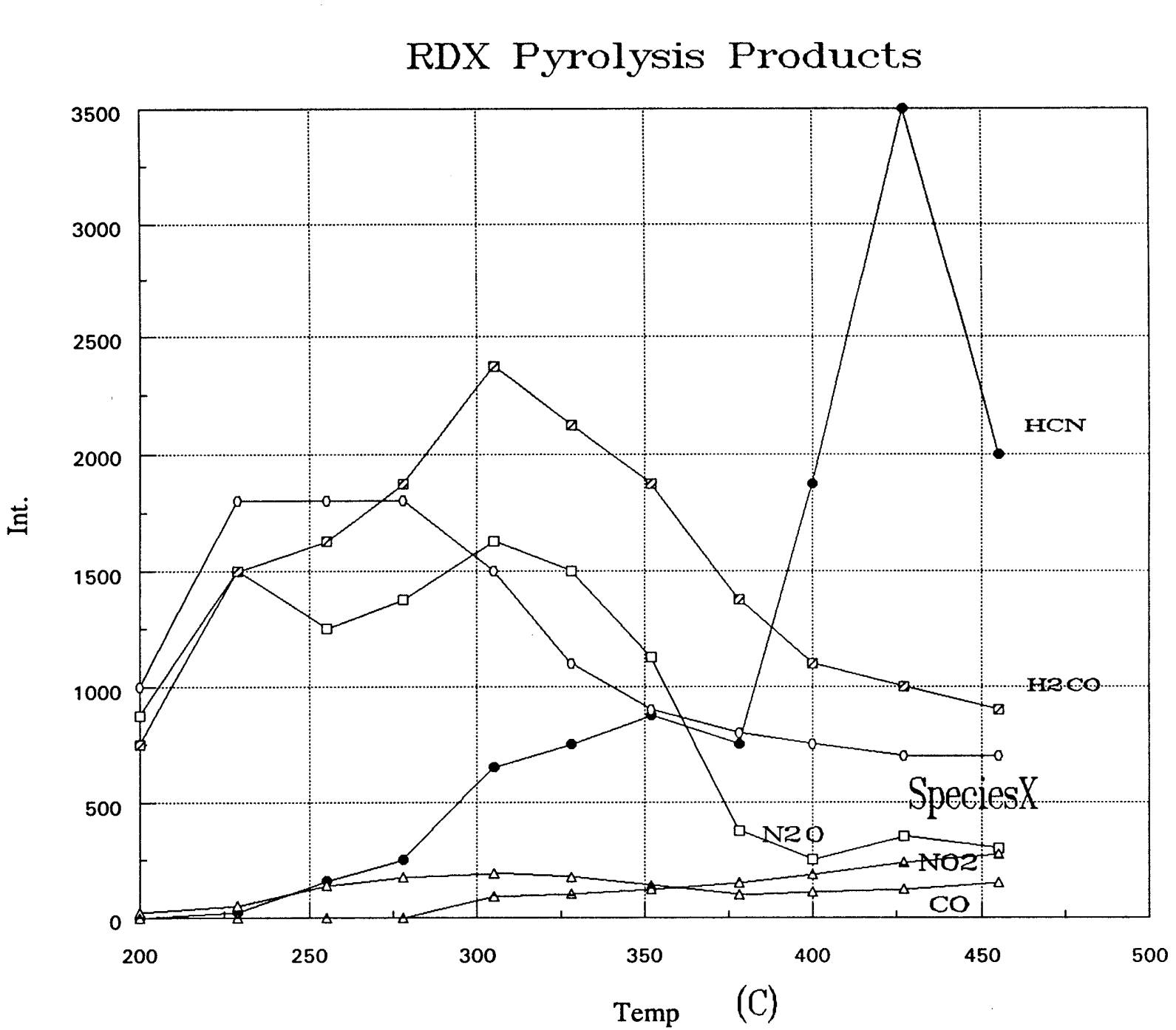
RDX Pyrolysis Products
Int.
3500
3000
2500
2000
1500
1000
500
0
200
250
300
350
400
450
500
Temp
(C)
HCN
H2CO
SpeciesX
N2O
NO2
CO

Fig c

TABLE I. Microwave Transitions Identified in Heated Nozzle FTMW Study of RDX

Frequency	Species	Transition	Comments
14488.47	H_2CO	2(1,1) -2(1,2)	S/N = 30
25123.30	N_2O	1 - 0	S/N = 40
23541.491	HONO	1(0,1) - 0(0,0)	S/N = 0.21
21982.097	HNCO	1(0,1) - 0(0,0)	S/N = 0.13
9237.027	NH_2CHO	3(1,2) - 3(1,3)	S/N = 0.13
15392.501	NH_2CHO	4(1,3) - 4(1,4)	S/N = 0.5
21207.234	NH_2CHO	1(0,1) - 0(0,0)	S/N = 0.7

TABLE II. Microwave Transitions Identified in Pyrolysis MW Study of RDX

Frequency	Species	Transition
66973.496	H_2CO	12(2,10)-12(2,11)
72409.097	H_2CO	1(0,1) - 0(0,0)
72838.948	H_2CO	5(1,4) - 5(1,5)
78230.50	H_2CO	21(3,18)-21(3,19)
116718.615	H_2CO	14(2,12)-14(2,13)
127154.96	H_2CO	23(3,20)-23(3,21)
145389.34	H_2CO	v_5
145603.64	H_2CO	2(02) - 1(01)
146635.3	$H_2{}^{13}CO$	2(02) - 1(01)
150400.72	H_2CO	v_5
75369.22	N_2O	3 - 2
125613.92	N_2O	5 - 4
125663.52	N_2O	5 - 4
125901.28	N_2O	5 - 4
125948.00	N_2O	5 - 4
125948.96	N_2O	5 - 4
53721.74	HCN	15 - 15
60861.65	HCN	16 - 16
68441.92	HCN	17 - 17
76461.46	HCN	18 - 18
84919.16	HCN	19 - 19
88630.416	HCN	1 - 0 F = 1 - 1
88631.847	HCN	1 - 0 F = 2 - 1
88633.936	HCN	1 - 0 F = 0 - 1
93813.84	HCN	20 - 20
103144.25	HCN	21 - 21
112909.10	HCN	22 - 22
65699.74	HNCO	3(1,3) - 2(1,2)
65946.17	HNCO	3(0,3) - 2(0,2)
65181.97	HNCO	3(1,2) - 2(1,1)
109498.34	HNCO	5(1,5) - 4(1,4)
109833.	HNCO	5(3) - 4(3)
109875.8	HNCO	5(2) - 4(2)
109908.95	HNCO	5(0,5) - 4(0,4)
109959.	HNCO	33(1,33) - 34(0,34)
113736.30	HNCO	43(0,43) - 42(1,42)
70588.6	NO_2	7(1,1) - 8(0,8)
70646.2	NO_2	7(1,1) - 8(0,8)
70654.1	NO_2	7(1,1) - 8(0,8)
150439.22	NO	3/2,3/2-1/2,3/2

TABLE II. Microwave Transitions Identified in Pyrolysis MW Study of RDX (CONTINUED)

Frequency	Species	Transition
109753.59	NH_2CHO	5(1,4) - 4(1,3)
127112.854	NH_2CHO	6(2,5) - 5(2,4)
127330.361	NH_2CHO	6(5) - 5(5)
127348.704	NH_2CHO	6(4) - 5(4)
127393.783	NH_2CHO	6(3,4) - 5(3,3)
127412.357	NH_2CHO	6(3,3) - 5(3,2)
128102.967	NH_2CHO	6(2,4) - 5(2,3)
148223.377	NH_2CHO	7(2,6) - 6(2,5)
148556.391	NH_2CHO	7(6) - 6(6)
148567.324	NH_2CHO	7(5) - 6(5)
148599.5	NH_2CHO	7(4) - 6(4)
148667.617	NH_2CHO	7(3,5) - 6(3,4)
148709.342	NH_2CHO	7(3,4) - 6(3,3)
149792.812	NH_2CHO	7(2,5) - 6(2,4)
98087.42	HONO	6(1,5) -6(0,6)
104237.45	HONO	7(1,6) - 7(0,7)
111551.60	HONO	8(1,7) - 8(0,8)
113841.170	HONO	5(1,5) - 4(1,4)
117281.36	HONO	5(0,5) - 4(0,4)
115271.207	CO	1 - 0
112287.11	HCOOH	5(2,4 - 4(2,30
112432.40	HCOOH	5(4) - 4(4)
112459.72	HCOOH	5(3,3) - 4(3,2)
112466.92	HCOOH	5(3,2) - 4(3,1)
112254.80	CH_3CHO	6(1,6) - 5(1,5) E

TABLE III. Species Identified by Mass Spectrometry and Microwave Spectroscopy

	Mass Spectrometry[1]	This Work
H_2O	yes	no line in range
HCN	yes	yes
CO	yes	yes
H_2CO	yes	yes
NO	yes	yes
N_2O	yes	yes
NO_2	yes	yes
HNCO	NO	yes
HONO	yes	yes
NH_2CHO	yes	yes
CH_3NHCHO	yes	NO
oxy-*s*-triazine	yes	spectrum unknown
ONDNTA[2]	yes	spectrum unknown
HCOOH	NO	yes
CH_3CHO	NO	yes?

1. Behrens & Bulusu, JPC **96**, 8877-8891 (1992).
2. 1-Nitroso-3,5-dinitrohexahydro-*s*-triazine

TABLE IV. Species X Rotational Parameters

Observed Transitions			Rotational Parameters	
Quantum Numbers	Obs. Freq.[a]	Obs.-Calc.[a]	Constant	Value[a]
2_{12}-1_{11}	70419.817	0.012	A (MHz)	141019.(58)
2_{02}-1_{01}	72801.475	-0.002	B (MHz)	19417.002(13)
2_{11}-1_{10}	75249.200	-0.003	C (MHz)	17002.124(12)
3_{13}-2_{12}	105605.596	-0.170	Δ_{JK} (kHz)	645.3(44)
3_{03}-2_{02}	109111.140	0.066	Δ_{J} (kHz)	36.43(43)
3_{22}-2_{21}	109238.000	0.047	δ_{J} (kHz)	5.60(34)
3_{12}-2_{11}	112848.900	0.038	ΔI (u$Å^2$)	0.113
4_{14}-3_{13}	140763.310	-0.155		
4_{04}-3_{03}	145311.620	-0.023		
4_{23}-3_{22}	145618.800	-0.033		
4_{13}-3_{12}	150418.140	0.000		
5_{15}-4_{14}	175884.350	0.099		

a. In MHz

TABLE V. Candidate molecular sources for Species-X

CC	CN	CO	NN	NO	OO
HCCH	HCN	HCO	HNN	HNO	HOOH
$CH_2=CH_2$	$CH_2=NH$	H_2CO	H_2NNH_2	H_2NOH	
CH_3CH_3	CH_3NH_2	CH_3OH			

Species	A (GHz)	B (GHz)	C (GHz)
Species-X	**141.0**	**19.42**	**17.00**
$CH_2=NH$	196.2	34.6	29.3
CH_3NH_2	103.1	22.63	21.71
H_2CO	281.9	38.8	34.0
CH_3OH	127.6	24.69	23.78
H_2NNH_2	143.4	24.08	24.07
H_2NOH	190.9	25.2	25.1
HNCO	918.5	11.07	10.9

APPENDIX 1. Spectral Line Survey of RDX Decomposition Products

Frequency	Intensity (μV)		
53 721.630	300	very slow +	
53 852	30		
53 962	30		
54 062	30		
54 097	40		
54 207	30		
54 310	40		
54 403	40	slow +	
54 931	30		
59 342.340	40		
59 929	30		
59 947	30		
60 285	30	slow +	
60 612	50		
60 861.600	260	very slow +	
65 232	30	-	
65 653	70		
65 880	40	-	
66 083	30		
66 249	30		
67 033	30	-	
67 218	70	+	
67 275	30		
67 833	40		
67 893	60		
68 286	30		
68 441.800	230	very slow +	
68 634	50	slow +	
68 752	60	slow +	
68 908	30		
69 384	40		
69 411	50	slow -	
69 442	40		
69 555	50		
69 613	50		
69 628	40		
70 364.640	30		
70 385.600	40		
70 419.800	500	very slow -	slow +
70 429.800	30		
70 603.300	30		
70 605.900	30		
70 620.700	40		
70 621.900	30		
70 640.660	40		
70 676.500	30		
70 706.100	30		
70 728.700	30		
70 731.900	50		
70 754.000	50		
70 760.600	50		
71 650.800	30		
71 669.220	70		
71 684.200	50		
72 801.740	260	slow + -	
75 249.190	900	very slow -	slow +
76 461.350	200	very slow +	
78 437	20		
78 876.930	30	+	
78 978	15		
79 004.820	130		
79 135.980	180		
79 232.700	30 \		
79 234.460	50 /		
79 249.160	30		
79 298.420	130		
79 338.570	170	broad	
79 363.260	130	+	
79 408.180	90		
79 411.980	70		
79 544.080	130		
79 560.760	60		
79 652.380	130		
79 656.420	170		
79 720.200	80		
79 744	25	?	
79 751.250	110	broad	
79 779.380	30		
79 789.560	100	broad	
79 795.860	60	+	
79 835.840	100		
79 852.120	70		
79 885.700	30		
79 917.480	180		
80 054.580	140		
80 116.540	130		
80 140.800	190	-	
80 169.450	100		
80 181.980	80		
80 190.740	30	slow -	
80 208.620	60		
80 220.020	50		
80 235.040	100		
80 291.320	30	slow -	
80 302.880	50		
80 313.660	130		
80 385.080	100		
80 405.500	60	broad	

80 414.780 40
80 420.160 60
80 421.900 40
80 433.120 40
80 477.620 60 \
80 479.780 60 /
80 609 50 +
80 843.060 70
80 860.780 80
81 212.740 60
81 241.560 160 \
81 242.760 120 /
81 255.600 95
81 283.760 150 -
81 368 30
81 415 40
81 488 30
81 491 35
81 568 30
81 571 30
81 627.220 60
81 629.600 60
81 807 20
81 871.620 40
81 876.870 45
81 901 20
81 934.650 40
81 941.900 20
81 946.430 30
81 973 25

82 008.440 60
82 029.540 110
82 058.760 60
82 075.900 50
82 145.180 60
82 165.780 50
82 182.240 40
82 283 40
82 298 40
82 348 120
82 402.420 40 slow -
82 418.160 70
82 470.360 110 slow -
82 481.100 40 slow +
82 487.980 110
82 623.800 30
82 670.160 60
82 681.100 50
82 789 40 slow -
82 821.500 110
82 890.340 50 slow +
82 946.560 40 -
82 964.380 100

83 063 70 +
83 505.440 80
83 701 40
83 860.360 120 -
83 894.400 110 slow -
83 940.320 100
83 995.680 60

84 168.475 80 -
84 205 60
84 234.530 90 -
84 524.820 60 very slow +
84 788 60 -
84 919.120 210 very slow +
84 966 80

85 101 100 +
85 245.700 100
85 265.660 100
85 612 50
85 637 50
85 759 60 -

86 655 70

87 197.830 60 +
87 619.670 45
87 677.590 40
87 729 60 slow -
87 737 30
87 757
87 767
87 821.900 60 slow +
87 886.850 70 broad

88 003.200 40
88 010.000 40
88 066.710 130
88 084.300 50
88 101 60
88 278 50
88 337.600 70
88 343.880 60
88 349.800 50 \
88 351.020 50 /
88 444.740 30 slow -
88 462.020 100
88 480.470 110
88 520.210 170
88 570.800 30
88 586.200 30
88 594.880 30
88 743.700 30

88 748.750 130
88 779.600 30 slow +
88 794.400 70
88 801.560 100
88 871.260 100
88 877.600 80
88 889.450 160
88 895.460 130
88 901.100 30
88 914.660 30
88 921.080 140
88 940.000 30
88 960.800 30

89 010.920 130
89 034.360 100
89 079.260 70
89 106.900 30
89 114.000 30
89 118.800 40
89 143.420 40 \ ?
89 144.050 40 / ?
89 191.160 220
89 211.800 30
89 258.600 30
89 279.620 240
89 329.670 220
89 359.880 180
89 377.860 130
89 388.660 110
89 426.180 130
89 438.780 160
89 443.760 30
89 455.400 190
89 474.700 30
89 505.900 30
89 515.620 170
89 551.560 40 + -
89 634.840 130
89 665.620 70
89 670.660 160
89 685.100 80
89 717.980 160

90 112.320 100 \
90 113.600 100
90 114.580 90 /
90 164.620 100
90 183.400 50 \
90 184.560 50 /
90 238.130 80
90 246.520 50 \
90 248.100 30
90 250.500 40
90 252.300 50 /
90 267.180 80
90 285.160 60 +
90 368.740 120
90 388.040 40
90 528.360 50
90 548.450 110
90 567.900 30 \
90 569.700 30 /
90 584.400 30 slow +
90 614.700 30
90 618.860 80
90 670.780 30
90 680.700 50
90 710.670 60
90 728.300 30
90 741.920 65 slow ? +
90 747.900 40
90 784.700 30
90 813.020 45
90 932 20

91 001.220 50
91 015.100 30
91 020.920 110
91 027.360 110
91 035.520 50
91 075.440 80 \
91 077.860 80
91 079.560 50 /
91 100.620 100
91 105.360 40 slow +
91 115.180 50
91 122.740 50
91 143.220 140
91 153.820 80
91 172.760 160
91 186.860 60 \
91 191.200 70
91 197.000 80 /
91 208.160 160 \
91 211.140 80 /
91 216.740 50
91 316.720 80
91 329.760 50
91 353.880 70 -
91 363.360 90
91 446.620 80
91 474.420 60
91 481.660 50
91 533.500 30 slow +
91 666.700 170
91 669.360 50
91 672.740 100

91 689.620 50
91 731.380 80
91 760.320 70
91 791.960 160
91 831.200 160
91 846.920 50

92 029.000 30
92 043.830 120 -
92 111.680 100
92 120.100 100
92 144.120 30 slow -
92 155.960 30
92 160.240 40 slow -
92 175.440 70
92 281.660 50
92 719 90
92 931 80
92 943 60

93 028 40
93 305.040 130
93 335.120 50 slow -
93 401 40
93 485.040 80
93 796 30
93 813.770 40 very slow +
93 843.480 110 slow -
93 909.580 30
93 920.960 30
93 926.860 30 slow-
93 935.500 30
93 952.800 60 slow +

94 035 40
94 144.800 40
94 172.400 100 slow -
94 210.600 80 slow -
94 354.580 60
94 389.780 50
94 435.460 140 slow -
94 479.820 130 slow -
94 706.040 110 +
94 837 50
94 909 40

95 169 40
95 312 90 +
95 362 90 slow -
95 606 90 broad
95 854 50 slow +
95 917 40 slow +

96 107 40 broad
96 372 100 slow +
96 520 90
96 635 100
96 802 120
96 807 60
96 994 40

97 042.240 180
97 135.160 40 slow -
97 149.400 100
97 158.780 110
97 300.600 130
97 319.840 60
97 408.080 100
97 427.540 100
97 432.340 90
97 539.400 110
97 579.640 60
97 640.800 100
97 677.620 30
97 777.500 60
97 883.920 60 \
97 885.240 50 /
97 896.340 60
97 906.500 40 \
97 907.980 40 /
97 920.380 50
97 928.920 50
97 929.720 290 \
97 934.200 290 } very slow +
97 941.800 210 /

98 001.620 110
98 013.960 70
98 023.620 130
98 031.160 30
98 086.840 30 slow +
98 107.520 140 \
98 120.960 140 } very slow +
98 134.800 140 /
98 246.500 30
98 275.600 80
98 278.920 30 \ slow -
98 281.120 20 slow -
98 283.400 7 / slow -
98 283.880 80
98 293.120 130
98 346.600 30
98 368.280 190 CH3CHO ?98 367.696
98 375.540 120
98 377.360 120
98 379.450 180
98 392.920 140 +
98 399.800 90

98 412.660 100
98 437.920 130
98 453.200 30
98 454.840 90
98 527.110 100 +
98 623.800 30
98 635.900 40 slow +
98 651.140 180
98 655.500 40
98 671.500 30 \
98 673.300 30
98 676.100 30 /
98 767.310 300 -
98 781.820 60
98 789.200 30
98 791.040 30
98 823.500 30
98 832.400 30
98 841.400 30
98 851.700 250
98 854.080 50
98 867.360 30
98 882.200 30
98 888.900 30
98 897.720 190

99 001.180 25
99 093 30
99 198.330 150
99 248 30
99 347.960 120
99 383.550 120
99 391.540 65
99 406.500 50
99 422.840 65
99 460.840 30
99 472.600 30 +
99 490.160 65
99 524.840 160
99 560.940 80
99 573.640 50 \
99 575.320 110 /
99 583.510 200
99 653.440 50
99 660.160 50
99 663.660 100
99 711.480 40
99 718.280 50
99 728.800 90
99 739.940 30 slow -
99 750.380 50 very slow -
99 765.360 90
99 769.300 140 \
99 771.120 170 /

99 804.140 100
99 825.220 40
99 838.940 70
99 877.780 140 \
99 881.120 130 /
99 902.640 130
99 905.440 50
99 924.820 50 \
99 926.020 70 /
99 955.100 100 +
99 965.040 90 \ -
99 968.480 60
99 970.660 70 /
99 995.440 90

100 002.800 40
100 004.640 60
100 011.220 40
100 014.360 100
100 027.780 60 +
100 053.320 60 \
100 054.780 45
100 055.900 45 /
100 063.330 130
100 070.660 80
100 087.960 30
100 129.780 50 CH3CHO 100 130.239
100 133.290 60
100 144.040 40
100 146.160 90
100 156.890 60 -
100 175.480 50
100 184.330 210
100 218.140 80 \
100 220.780 80
100 224.560 50 /
100 234.620 100
100 242.300 40 \
100 245.120 60
100 247.840 50 /
100 324.860 90
100 341.320 80
100 351.200 130 \
100 353.000 60 /
100 363.400 80 \
100 366.620 60 /
100 384.380 80
100 469.060 40
100 474.620 100
100 479.800 50 \
100 482.040 60 /
100 506.180 90
100 517.520 60
100 524.280 85

100 526.480 40
100 610.560 140 \
100 612.540 130 /
100 616.820 100 slow -
100 638.760 60
100 646.440 100
100 650.180 80
100 674.260 180
100 708.580 170
100 759.380 90
100 775.920 60
100 777.880 150
100 781.900 40
100 878.600 80
100 892.350 60
100 901.050 40
100 908.150 40
100 922.750 40
100 938.750 50 NH2CHO 100 922.291
100 952.300 130
100 960.880 250

101 120.130 170
101 258.160 130
101 341 70
101 375.660 210
101 456.810 160
101 541 90
101 678 60
101 711.010 90
101 787.930 130
101 820 90

102 052 40
102 064.230 80 NH2CHO 102 064.3
102 203 70 -
102 308.070 130
102 567.320 30 slow -
102 682.620 50 slow +
102 934.180 40 slow -
102 958 90

103 008.910 100
103 223.400 50 slow +
103 448.280 100 slow -
103 642 60 slow -
103 808 50
103 821 50

104 091 50
104 119 50
104 237 100 +
104 286 70
104 398 100
104 528.050 50 very slow +
104 557 70
104 583 60 broad
104 590 40 slow +
104 814 90 slow +

105 098 90
105 246 90
105 258 100
105 354.100 40 -
105 385.900 320
105 543.340 520 +
105 605.590 100 slow +
105 625.600 60 slow +
105 653.000 320
105 665.030 40 \
105 666.240 60 /
105 754.830 600 - + 50 V
105 773.680 200
105 775.700 50
105 800.600 50
105 810.060 30 \
105 812.400 30 /
105 817.560 50
105 832.340 240
105 877.420 50
105 891.710 270 +
105 910.520 320
105 946.800 100 slow +
105 957.600 40
105 972.540 260

106 023.160 50 slow -
106 067.480 210 \
106 069.490 210 /
106 093.520 250
106 096.180 50
106 107.720 110
106 134.780 60
106 141.000 70
106 146.200 140
106 151.860 100
106 172.240 210
106 183.860 40
106 300.200 290
106 307.180 130
106 358.600 40
106 396.820 70
106 409.500 130
106 513.320 140 +
106 533.700 190
106 541.580 140
106 569.340 40 -
106 600.240 160

106 606.300 130 \
106 608.260 100 /
106 715.330 160 \
106 718.100 130 /
106 751.820 220
106 897.500 110
106 914.420 180
106 971.580 60
107 013.820 45 CH30H 107 013.85
107 017.780 75 + -
107 023.790 50
107 034.590 270 +
107 036.840 25
107 041.740 40
107 044.620 40
107 045.600 30
107 057.110 160
107 107.770 230
107 123.320 190
107 175.460 30
107 178.960 30
107 182.330 180
107 195.370 130 +
107 232.560 100
107 243.680 170 \
107 245.010 160 /
107 364.620 40
107 367.280 110
107 372.860 30
107 376.020 30
107 377.090 110
107 419.570 20 slow -
107 448.280 60
107 494.240 140
107 499.420 80 \
107 500.560 60 /
107 559.510 100
107 582.110 90 -
107 619.800 160
107 746.040 50
107 797.340 130
107 814.940 50
107 845.700 150
107 870.520 160
107 904.630 250
107 949.920 100
107 956.490 230
107 973.200 60
107 989.320 40 slow +

108 010.540 25
108 014.780 15
108 028.930 65
108 238 90
108 245.200 80 +
108 408.810 140
108 418.360 50
108 454.520 60
108 492.890 130
108 589.740 25 \
108 590.600 15 /
108 609.210 20
108 704 50
108 740.720 90 +
108 748.540 30
108 797.380 100
108 804.300 45
108 809.760 25
108 822.510 40
108 857.940 40
108 919.760 160
108 937.100 30
108 943.300 100 \
108 944.690 100 /
108 959.820 100 \
108 960.360 100 /
109 009.880 30 -
109 019.890 60 +
109 031.040 130 \
109 031.740 130 /
109 040.910 130
109 048.640 130
109 072.210 100
109 105.870 40 \
109 108.050 40 /
109 115.140 50
109 121.480 40
109 126.610 20
109 127.680 50
109 138.720 35 CH3OH 109 138.71
109 149.850 40
109 162.900 30 slow +
109 187.050 50 \
109 188.250 50 /
109 194.900 40 slow -
109 198.720 20
109 209.450 50
109 238.080 60 ?
109 263.400 100
109 269.950 50
109 274.500 40
109 278.240 40
109 283.400 40 -
109 361.800 50 slow -
109 367.750 40
109 372.250 30
109 375.870 50 \
109 377.050 40

109 380.500 40 /
109 482.560 30 slow +
109 538.620 50
109 547.350 40
109 553.360 60 slow +
109 556.690 35
109 604.660 60 slow -
109 640.050 100
109 692.980 45
109 776.480 60 \
109 779.540 80 /
109 785.340 50
109 806.940 50 \
109 807.900 60 /
109 824.660 40
109 890.880 50
109 905.580 70 slow +
109 956.140 30
110 030.460 80
110 089.140 160
110 104.720 80
110 110.920 100
110 156.900 30
110 164.240 40
110 254.920 130
110 418.960 110
110 460.980 290
110 523.580 30
110 548.540 210
110 619 60 -
110 855 50
110 948 50 slow +
111 028.770 40
111 047.550 40 broad
111 133 60
111 285 60
111 319.480 40
111 328.940 40
111 336.240 40
111 365.860 40
111 367.860 130
111 384.070 260 -
111 402.420 60 slow -
111 474.420 30 slow +
111 497.480 130
111 514.590 170
111 540.660 40 slow +
111 551.150 30 slow + ?
111 723 20
111 806.290 190 -
111 899.300 240 -
111 917.140 30 slow -
111 923.860 40 slow +
111 982.190 50 very slow -
112 105.060 110 \ -
112 105.560 110 /
112 114.860 180 -
112 254.800 230 CH3CHO 112 254.48 6(1,6) - 5(1,5) E
112 287.110 100 HCOOH 112 287.12 5(2,4) - 4(2,3)
112 382.950 70
112 432.400 100 HCOOH 112 432.30 5(4,2) - 4(4,1)
112 459.720 100 HCOOH 112 459.60 5(3,3) - 4(3,2)
112 466.920 100 HCOOH 112 467.00 5(3,2) - 4(3,1)
112 469.240 60
112 543.670 70 slow -
112 545.610 40
112 567.750 30 slow +
112 586.360 110 \
112 587.460 70 /
112 714.980 90 slow +
112 727.560 70 broad
112 775.500 35
112 848.900 350 slow -
112 860.800 30
112 891.440 50 HCOOH 112 891.41 5(2,3) - 4(2,2)
112 896.080 80
112 899.120 40
112 926.390 70 slow -
112 938.370 190 \slow -
112 941.850 130 /slow -
113 083 30 -
113 108.920 160
113 111.720 160 slow -
113 157 60
113 162 50
113 232.000 70
113 321.979 90
113 323.530 100
113 379.100 90
113 430.130 90 slow +
113 492.410 90
113 580 60 slow -
113 660 90 slow +
113 705 40 slow +
113 736 90 slow +
113 786 70
113 841.170 45 slow + HONO 113 841.03 5(1,5) - 4(1,4)
114 003.820 20 \slow +
114 005.340 45 slow +
114 006.940 7 /slow +
114 019.200 30
114 034.000 50
114 043.160 200
114 058.590 210
114 069.080 30
114 123.790 260
114 134.940 50
114 141.220 30

114 148.700 80 \
114 149.640 40 /
114 166.400 40
114 233.020 50 -
114 278.150 350
114 312 50 broad
114 408.960 100 broad
114 471.280 160 slow -
114 534.600 40 broad
114 576.380 260
114 582.860 70 broad
114 589.500 30
114 598.240 230
114 602.520 70
114 643.920 30
114 650.880 30
114 662.700 100
114 727.400 260
114 736.370 150
114 748.000 200 \
114 749.160 200 /
114 750.560 40 CH3OH 114 750.70
114 764.940 40
114 786.980 170
114 803.120 110
114 806.620 30
114 816.020 80 \
114 818.700 50
114 832.840 30
114 843.350 180
114 890.300 30
114 893.780 40 slow +
114 903.770 60 slow -
114 906.900 50
114 975.580 30
114 996.290 190
115 019.130 160
115 036.920 70
115 061.660 90
115 063.170 20
115 070.780 200
115 106.330 65
115 110.810 200
115 119.750 200
115 144.120 65
115 146.740 200 slow -
115 155.180 200
115 203.850 260
115 291.540 20 \slow +
115 293.540 25 slow +
115 295.520 15 /slow +
115 338.220 160 \
115 339.960 320 /
115 410.120 100
115 426.300 60
115 434.570 200
115 462.540 50
115 563.040 30
115 628.420 140
115 634.620 80 slow +
115 710.560 15 \slow +
115 711.640 15 slow +
115 712.720 15 /slow +
115 716.520 170
115 725.860 140 C2H5CN-? 115 725.965
115 734.210 160
115 804.740 90 slow +
115 810.300 30
115 815.880 140
115 843.800 40
115 846.760 110
115 856.400 100
115 881.500 140
115 892.060 60
115 902.440 50
115 924.960 80
115 934.860 65
115 938.380 50
115 960.220 290 \
115 962.900 140 /
115 971.180 90
116 119.600 130
116 161.390 270
116 173.010 100
116 176.870 280 \
116 178.020 250 /
116 235.590 280
116 238.160 260
116 241.340 260
116 309.500 40
116 340.050 90
116 345.750 30
116 378.050 30
116 388.100 30
116 412.080 180
116 447.470 120
116 514.050 170
116 565.170 160
116 618.320 100 \
116 619.610 90 /
116 646.720 20 \
116 647.570 100 /
116 711.440 15 CH3CHO 116 711.450
116 715.270 150
116 725.650 160
116 757 60 +
116 786.080 120
116 922.500 50

116 953.750	25	
117 137.360	50	
117 143.060	80	
117 149.600	60	
117 225.700	50	
117 281.700	70	slow -
117 383.050	210	
117 436.770	90	
117 467.710	180	
117 514.420	180	
117 602.290	25	
117 605.600	30	
117 615.300	30	
117 626.600	30	
117 630.200	40	
117 641.000	30	
117 651.940	50	
117 678.420	100	
117 738.700	50	
117 741.200	60	
117 760.200	60	+ -
117 766.360	50	
117 769.880	30	
117 777.000	30	
117 816.520	80	
117 831.890	170	
117 842.380	80	
117 847.220	80	slow +
117 870.980	80	
117 903.000	80	
117 911.760	40	
118 003.280	70	
118 006.420	70	
118 026.610	50	
118 039.100	70	
118 070.770	40	
118 078.310	50	
118 086.470	50	
118 092.200	7	CH3CHO 118 092.403
118 093.840	40	
118 098.440	50	\
118 099.640	50	/HCOOCH3 118099.557
123 508	40	
123 648	40	
123 789	90	broad
124 085	80	
124 253	80	
124 306	80	
124 424	80	
124 455	80	
124 511	90	
124 905	90	
124 927	80	
124 948	80	
125 035.520	80	
125 062.940	120	
125 215	80	
125 318	100	
125 538	80	2 lines
125 684	100	
125 819	70	
125 887	80	
127 553	80	
131 155	50	
131 353	60	
131 508	90	+
131 618	40	slow +
131 628	70	
131 751	60	
131 813	90	
131 920	70	
133 545	90	
133 556	100	broad
133 644	100	broad
133 712	60	-
133 722	80	
134 105.020	80	
134 131.260	110	
134 139.980	190	\
134 142.300	200	/
134 165.700	80	slow -
134 201.880	200	\
134 204.300	250	/
134 256.220	100	
134 280.220	150	
134 348		100
134 409.800	80	\
134 414.600	80	/ broad
134 436.000	200	slow +
134 468.800	100	
134 481.520	450	very slow HNCO
134 565	80	
134 606.400	70	slow -
134 642.320	90	
134 676.080	90	
134 713.120	70	broad
134 720.420	80	
134 784.100	140	
134 788.880	160	
134 815.900	50	
134 830.000	130	
134 842.340	260	

134 870.980	200	
134 968.640	220 \	-
134 971.620	100 /	
134 980.440	200	
135 101	150	
135 356	200	
135 394	150	
135 443	100	
135 597	150	
135 612.100	80	broad
135 618.300	80	
135 648.440	100	
135 682.440	130	
135 705	60	
135 738	60	
135 772	90	
135 895	60	
136 210	90	
136 234	80	
136 466	60	
136 497	60	
136 550	50	+
136 594	60	
136 644	80	
140 721.180	60	
140 735.000	70	
140 752.800	150	
140 763.310	1300	
140 808	130	
142 015	70	
142 030	70	
142 112	60	
142 129	60	
142 228	80	
142 414	80	
142 502	70	
142 511	130	
142 736	60	
142 740	60	
142 746	60	
142 838	70	
142 845	80	
142 860	80	
142 883	90	
142 896	70	
143 108	60	
143 436	80	
143 454	80	
143 517	60 \	
143 519	60 /	
143 577	100	
143 582	100	
143 589	90	
144 133	90	
144 272	70	
144 439	60	
144 483	60	
144 681	70	
144 827.920	150 \	slow ?
144 833.900	80 /	slow ?
144 906	100	
145 116	100	
145 225	150	
145 370.000	70	
145 389.700	250	H2CO nu5
145 450.600	80	
145 459.740	80	
145 477.300	130	
145 481.240	130	very slow +
145 505.420	60	
145 519.660	60	
145 535.220	90	
145 551.180	80	
145 563.900	180	
145 574.180	200	
145 618.930	150	
145 650.260	500	slow +
145 664.400	150	
145 681.300	80	
145 685.820	80	
145 703.780	60	
145 710	90	
145 715	90	
145 732.500	80	
145 749.140	80	
145 762.300	90	
145 766.180	100	
145 769.900	90	
145 789.900	100	
145 792.520	150	
145 811.400	70	
145 819.520	80	
145 826.600	100	
145 836.400	100	
145 839.840	400	very slow +
145 910.500	40	+
145 937.000	60	
145 943.400	100 \	
145 946.220	100	
145 947.540	100 /	
145 962.940	100	

145 971.220	30	-
145 973.900	30	
145 983.200	60	
145 988.540	60	
146 145.200	100	slow +
146 167.400	50	
146 175.640	60	
146 186.000	50	
146 507	70	
146 581	60	
146 686	60	
146 679	70	
146 673	50	
146 734	90	
146 837	80	
146 855	80	
146 862	80	
146 981	70	slow +
147 209	60	
147 239	60	
147 329	130	
147 476	100	
147 566	90	
147 590	70	
147 596	70	
147 618	100	
147 691	80	
147 761	200	
147 879.740	200	-
148 069	90	
148 157	80	
148 347	80	
148 350	80	
148 544	70	
148 578	80	
148 598	70	
148 667	60	
148 696	70	
148 783	60	
148 993	150	
149 031	70	
149 086	70	
149 137	70	+
149 163	60	+
149 225	100	
149 234	100	
149 342	60	
149 381	100	
149 409	100	
149 607	70	
149 820	100	
149 928	150	-
150 021	150	
150 094	190	
150 129.820	130	-
150 141.600	40	
150 150.000	300	
150 156.960	400	
150 206.800	70	
150 235.200	70	
150 268.720	70	
150 280.020	100	
150 297.080	240	
150 320.700	50	
150 330.000	60	
150 341.120	300	
150 383.840	100	
150 418.125	600	
150 522.380	180	
150 562.240	100	
150 575.040	200	
150 600.620	150 \	
150 602.180	150 /	
150 626.340	200	
150 787.400	60	slow -
150 793.860	150	
150 794.820	110	very slow +
150 998	150	
175 884.325	120	slow